

충격하중을 받는 Euler기둥의 동적좌굴 해석

Dynamic Instability Analysis of Euler Column under Impact Loading

김 형 열*
Kim, Hyeong-Yeol

요 약

Explicit 직접적분법 알고리즘을 사용하여 Euler 기둥의 동적 좌굴거동을 해석할 수 있는 수치해석법을 제시하였다. 평면뿔대 유한요소를 기하학적 비선형 거동과 전체좌굴의 영향을 고려할 수 있도록 보의 대변위 이론으로부터 유도하였고, central difference method를 바탕으로 해석 알고리즘을 개발하였다. 다양한 형상, 크기, 재하시간을 갖는 충격하중에 대하여 Euler기둥의 동적좌굴거동과 고유치 문제를 해석하였다. 수치해석예제를 통하여 본 연구의 결과를 검증하였다.

Abstract

An explicit direct time integration method based solution algorithm is presented to predict dynamic buckling response of Euler column. On the basis of large deflection beam theory, a plane frame finite element is formulated and implemented into the solution algorithm. The element formulation takes into account geometrical nonlinearity and overall buckling of steel structural frames. The solution algorithm employs the central difference method. Using the computer program developed by the author, dynamic instability behavior of Euler column under impact loading is investigated by considering the time variation of load, load magnitude, and load duration. The free vibration of Euler column caused by a short duration impact load is also studied. The validity and efficiency of the present formulation and solution algorithm are verified through illustrative numerical examples.

Keywords : buckling, column, finite element method, impact load, dynamic buckling

1. INTRODUCTION

In nonlinear load-deflection analysis of structural stability problems, the difficulty is enhanced when dynamic loading is considered. This

is because the currently available finite element solution procedures for nonlinear dynamic analysis are generally based on the implicit direct integration methods. This method requires a great deal of additional computa-

* 정회원 · 한국건설기술연구원 구조연구실 선임연구원

• 이 논문에 대한 토론을 1996년 12월 31일까지 본 학회에 보내주시면 1997년 6월호에 그 결과를 게재하겠습니다.

tional effort in assembling the structure stiffness matrix and solving the resulting simultaneous linear equations for every time step. For this reason, the implicit method becomes inefficient, especially for nonlinear transient analysis problems.¹⁾ In addition, due to ill-conditioning of the stiffness matrix, this type of finite element formulation is susceptible to numerical difficulties in certain cases of structural instability problems.

An alternative solution procedure, namely the explicit direct time integration method shown to be a simple but efficient solution procedure to predict accurately and efficiently the transient response of structures.²⁾ Unlike the implicit method, being free of numerical ill-conditioning, most explicit methods can be carried out until the progressive structural failure of the structure occurs. It is noted, however, that a major drawback of the explicit method is in its inefficiency in inducing viable static solutions.

In this paper, an efficient dynamic buckling analysis solution algorithm has been developed for progressive instability analysis of columns. The explicit direct integration method is utilized to overcome the difficulty in nonlinear dynamic analysis. On the basis of large deflection beam theory, a plane frame element is formulated. The two node element possesses three degrees of freedom per node. Using the explicit method of solution algorithm, a computer code is developed, and its validity is verified through illustrative examples. Dynamic buckling behavior of a geometrically perfect pin-ended column, which refers to as Euler column herein, under impact loading is investigated. Dynamic loading parameters which play an important role in predicting the buckling response of Euler column are identified.

2. DESCRIPTION OF ANALYSIS PROCEDURE

The overall solution algorithm developed in this study is based on a solution methodology which refers to as the predictive structural analysis procedure.¹⁾ The analysis procedure is predictive in nature because the realistic response of structures is described in a step-by-step manner as the time is increased and the load is incremented.

Throughout the analysis process, a load is applied to a structure in increments. At each prescribed step of loading, the structure reaches a new equilibrium condition and the desired information describing the behavior of the structure is obtained. Then, additional load is applied to the updated structural configuration, and the same process is repeated. This iterative procedure continues until complete structural collapse occurs due to either excessive material failure or structural instability.

2.1 Description of Solution Algorithm

In the conventional implicit method based structural stability analysis, a matrix that accounts for the change in potential energy associated with the element rotation, which is usually referred to as the geometric stiffness matrix,³⁾ is required and added to the governing matrix equation of the idealized structural system. For nonlinear structural stability analysis, the geometric stiffness matrices are usually a quadratic function of the displacement. Hence, the formulation of geometric stiffness matrix requires the solution of governing matrix equation.

In this study, on the other hand, the geometric internal force vector due to the change in geometry is explicitly calculated, and added to the internal force vector of the structure.

During the course of loading, the magnitude of the geometric internal force vector is small, and its effect on the behavior of a structure may be insignificant. However, when the external load approaches its critical value, the geometric internal force vector becomes significant, and structural instability occurs.

In this study, structural instability is predicted using the load-deflection method of analysis. By examining the maximum structural response obtained for the current and preceding load steps, if a relatively small increase in load causes large value of deflection, the structural instability is assumed to occur. Then, the previously carried load value is considered as the ultimate load carrying capacity of the structure. At the end of solution process within the current load increment, the maximum displacement in the structure is determined. If the difference between maximum displacements computed at the current and preceding steps is greater than the prescribed tolerance limit, the structure is assumed to be failed by buckling. Otherwise, the structural geometry and degrees of freedom are updated for the next time step, and the solution process is advanced with the next time step.

2.2 Solution to Equation of Motion

A general form of the differential equation of motion of an idealized structure can be semi-discretized using the finite element method with respect to space coordinates, and written in matrix form as^{3,4)}

$$[M]\{\ddot{D}\} + [C]\{\dot{D}\} + [K]\{D\} = \{F_{ex}\} \quad (1)$$

where $[M]$, $[C]$, and $[K]$ are the mass, damping, and stiffness matrices of the structure, respectively. $\{D\}$ is the nodal displacement vector, and $\{\dot{D}\}$ and $\{\ddot{D}\}$ are the corresponding no-

dal velocity and acceleration vectors of the structure, respectively. $\{F_{ex}\}$ is a time dependent external force vector of the structure.

In order to reflect the time dependent nature of the problem, by denoting the current and previous time steps by $t+\Delta t$ and t , respectively, the semi-discretized matrix equations of motion in Eq. 1 can be rewritten as

$$[M]\{\ddot{D}\}^{t+\Delta t} + [K]\{D\}^t = \{F_{ex}\}^{t+\Delta t} \quad (2)$$

It is noted that an arbitrary damping effect is excluded in the above expression. $[M]$ is assumed to be time independent.

In the direct time integration methods, the space discretized matrix governing equation of a structure is solved by using either the implicit direct time integration method or the explicit direct time integration method. In the implicit method, the information at the current time step is obtained by iteratively adjusting the governing equation until internal and external equilibrium conditions are satisfied for that step. Whereas in the explicit method, the information at the current time step is obtained by directly solving the equation of motion at the previous time step. Hence, the solution of explicit method is obtained in a rather explicit and direct manner.

For small finite element models, $[k]$ can be formed and the internal force vector at each time step can be computed by $\{f_{in}\} = [k]\{d\}$, in which $[k]$ and $\{d\}$ are the stiffness matrix and nodal displacement vector of the element, respectively. On the other hand, in explicit method the internal force vector can be computed by summation of element contributions.

In explicit method of formulation, the element internal force vector can explicitly be calculated by⁴⁾

$$\{f_{in}\}^t = \int_V [B]^T \{\sigma\} dV \quad (3)$$

where $[B]$ is the element strain-displacement relation matrix, $\{\sigma\}$ the element stress vector, and V the volume of the element. Hence, in explicit method, the governing matrix equation of structural system in Eq. 2 can be rewritten as

$$[M]\{\ddot{D}\}^{t+\Delta t} = \{F_{ex}\}^{t+\Delta t} - \{F_{in}\}^t \quad (4)$$

in which $\{F_{in}\}$ is the internal force vector of the structure.

Knowing the structural external force vector at the current time step, the structural nodal acceleration vector can explicitly be computed as

$$\{\ddot{D}\}^{t+\Delta t} = [M]^{-1}(\{F_{ex}\}^{t+\Delta t} - \{F_{in}\}^t) \quad (5)$$

To obtain the solution, it is necessary to integrate Eq. 5 twice through the time space. The most commonly used operator in the explicit method is the central difference operator.²⁾ In this study, the equations of motion are integrated explicitly in time by the central difference method, in which the structural nodal velocity and displacement are computed as³⁾

$$\{\dot{D}\}^{t+\Delta t} = \{\dot{D}\}^t + \frac{1}{2}\Delta t[\{\ddot{D}\}^t + \{\ddot{D}\}^{t+\Delta t}] \quad (6)$$

and

$$\{D\}^{t+\Delta t} = \{D\}^t + \Delta t\{\dot{D}\}^t + \frac{1}{2}\Delta t^2\{\ddot{D}\}^t \quad (7)$$

In the above, the structural nodal degrees of freedom are obtained without solving simultaneous equations, which is necessary in the implicit method. Since the structural stiffness matrix need not be formed or stored, the explicit method can treat large scale problems

with comparatively modest computer storage requirements.

In all cases of problems, the explicit method requires numerical integration along the loading path at high precision. Thus, many steps of numerical integration are always required. Major disadvantage of the explicit method compared to the implicit method is that the explicit method requires very small time step for numerical stability requirements. Furthermore, $\{F_{in}\}$ is needed to be recalculated at every time step even though the stiffness matrix is not changed. Therefore, the explicit method is suitable for only some special class of problems such as transient analysis of nonlinear problems.¹⁾

3. FORMULATION OF PLANE FRAME ELEMENT

3.1 Element Description

In order to verify the proposed solution algorithm in predicting dynamic response of structures, a plane frame element is developed using the large deflection beam theory. The element consists of three degrees of freedom per node (Fig. 1). The two translational degrees of

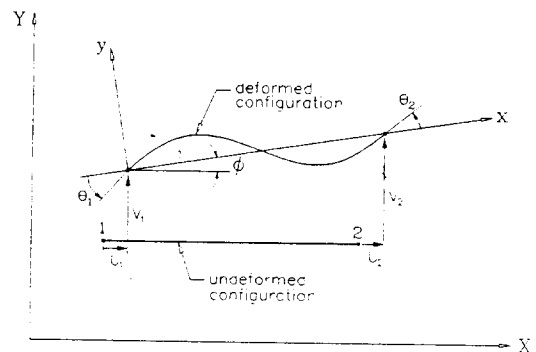


Fig. 1 Element deformation and rigid body rotation in local and global coordinates

freedom are denoted by u , v , and the rotational degree of freedom denoted by θ .

On the basis of updated Lagrangian formulation, the element is formulated in the local coordinates. The nodal displacement vectors $\{d\}$ and $\{D\}$ in the local and global coordinates are defined, respectively, as

$$\{d\} = [u_1 \ v_1 \ \theta_1 \ u_2 \ v_2 \ \theta_2]^T \quad (8)$$

and

$$\{D\} = [U_1 \ V_1 \ \Theta_1 \ U_2 \ V_2 \ \Theta_2] \quad (9)$$

The conditions imposed in the local nodal displacement vectors are

$$u_1 = U_1 - U_1 = 0 \quad (10a)$$

$$u_2 = U_2 - U_1 \quad (10b)$$

$$v_1 = V_1 - V_1 = 0 \quad (10c)$$

$$v_2 = V_2 - V_1 \quad (10d)$$

$$\theta_1 = \Theta_1 - \phi \quad (10e)$$

$$\theta_2 = \Theta_2 - \phi \quad (10f)$$

where ϕ is the rigid body rotation of the element as illustrated in Fig. 1.

3.2 Displacement Functions

For the displacement components in Eq. 8, the conventional displacement functions for the frame element are assumed. Assuming the axial displacement to be linear in the x direction, the axial displacement in terms of local nodal displacement can be written as

$$u = \frac{x}{L_e} u_2 \quad (11)$$

where L_e is the length of the element. The transverse displacement is assumed to be a cubic function as

$$v = \theta_1 x - (2\theta_1 + \theta_2) \frac{x^2}{L_e} + (\theta_1 + \theta_2) \frac{x^3}{L_e^2} \quad (12)$$

For the assumed cubic transverse displacement field in Eq. 12, the rotational displacement is obtained as

$$\theta = \frac{\partial v}{\partial x} = \theta_1 - (4\theta_1 + 2\theta_2) \frac{x}{L_e} + 3(\theta_1 + \theta_2) \frac{x^2}{L_e^2} \quad (13)$$

It should be noted that the transverse shear deformation of the element is neglected in Eq. 13. The previous research⁵⁾ indicated that shear deformation has little effect on the buckling response of columns.

For the calculation of rigid body rotation of the element, the following assumption is made. Although rotation may be arbitrarily large, the deformation itself is small. Hence, the rotation relative to the x -axis must be small, so that the angle of rotation of the x -axis is a good approximation to the rigid body rotation of the entire element.²⁾ In this study, the rigid body rotation within the element is approximated by the following relationship.

$$\phi = \sin^{-1} \left[\frac{L_o \times L_n}{L_o L_n} \right] \quad (14)$$

where L_o and L_n are the vectors, which represent the original and deformed length of the element, respectively. \times represents vector product.

3.3 Calculation of Element Internal Force Vector

In the following, according to the principle of virtual work, the element internal force vector is derived.

The strain-displacement expression employed in structural instability problem must in-

clude the geometric nonlinear strain term, and is given by⁶⁾

$$\varepsilon = \frac{\partial u}{\partial x} - y \frac{\partial^2 v}{\partial x^2} + \frac{1}{2} \left(\frac{\partial v}{\partial x} \right)^2 \quad (15)$$

Using the kinematic relationships in Eq. 15 and a linear-elastic constitutive relationship, the change in internal work of the element can be written as

$$\begin{aligned} \delta W_{in} = & \delta \int_0^{L_e} \left[\int_A \frac{\partial u}{\partial x} \sigma dA - b \int_y \frac{\partial^2 v}{\partial x^2} y \sigma dy \right. \\ & \left. + \frac{1}{2} \int_A \left(\frac{\partial v}{\partial x} \right)^2 \sigma dA \right] dx \end{aligned} \quad (16)$$

where A is the cross-sectional area and b the width of the element.

Using the element internal force vector in Eq. 3, and denoting the virtual nodal displacement as $\{\delta d\}$, the variation of internal work also can symbolically be written as⁴⁾

$$\delta W_{in} = \{\delta d\}^T \{f_{in}\} \quad (17)$$

With the aid of Eq. 17, the change in internal work due to axial deformation in Eq. 16 can be rewritten as

$$\delta W_{in}^1 = \{\delta d\}^T \int_0^{L_e} [B_1]^T \{\sigma\} A dx \quad (18)$$

where $[B_1]$ is the strain-displacement relation matrix, which is corresponding to the axial deformation in Eq. 11. By comparing Eq. 17 with Eq. 18, the internal force vector due to the axial deformation is defined as

$$\{f_{in}^1\} = \int_0^{L_e} [B_1]^T \{\sigma\} A dx$$

Similarly, the change in internal work due to bending in Eq. 16 can be rewritten as

$$\delta W_{in}^2 = \{\delta d\}^T \int_0^{L_e} \int_y b y [B_2]^T \{\sigma\} dy dx \quad (20)$$

where $[B_2]$ is corresponding to the transverse

displacement in Eq. 12.

In the same manner, by comparing Eq. 17 with Eq. 20, the internal force vector due to the bending is defined as

$$\{f_{in}^2\} = \int_0^{L_e} \int_y b y [B_2]^T \{\sigma\} dy dx \quad (21)$$

The change in internal work due to the change in geometry is integrated numerically at points $x=0$ and $x=L_e$ within the element. The result is shown in the following.

$$\delta W_{in}^3 = \delta \theta_1 P_{in} \theta_1 L_e + \delta \theta_2 P_{in} \theta_2 L_e \quad (22)$$

where P_{in} is the internal axial force, which is numerically integrated over the cross-sectional area of the element. With the aid of Eq. 17, the internal force vector due to the change in geometry, which is referred to as the geometric internal force vector, $\{f_{in}^3\}$, can be defined. In the present study, the geometric internal force vector is computed and added to the element formulation, which aims to take into account the structural instability effect.

The internal force vector of the element, $\{f_{in}\}$, is the sum of the three internal force vectors, $\{f_{in}^1\}$, $\{f_{in}^2\}$, and $\{f_{in}^3\}$.

3.4 Calculation of Element Mass Vector

In this study, the lumped element mass vectors are explicitly calculated using the lumped mass approach⁴⁾, and result is shown in the following.

$$\{m\} = \frac{1}{2} \rho A L_e \left\{ 1 \quad 1 \quad \frac{L_e^2}{12} \quad 1 \quad 1 \quad \frac{L_e^2}{12} \right\}^T \quad (23)$$

where is the mass density of the material.

4. ILLUSTRATIVE NUMERICAL EXAMPLES

In order to validate the present formulation

and solution algorithm, selected example problems are solved by the computer program developed in this study,⁷⁾ and the solutions are compared with the analytical solutions. A typical example of buckling of structures may be an initially straight column with pin-ended support under axial load, which known as Euler column(Fig. 2). The time step used in the calculation is $t=4 \times 10^{-6}$ sec, which satisfies the numerical stability requirement for the central difference method. The finite element model used in the analysis is composed of 10 frame elements. The integration points used in the analysis are two and five for the element length and depth directions, respectively. For the simplification, damping effect is neglected throughout the numerical analysis.

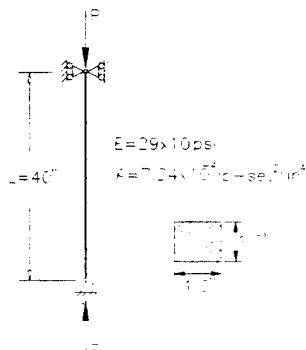


Fig. 2 Configuration, loading, and support conditions of column

4.1 Euler Column under Static Loading

In the first example, the buckling behavior of Euler column under static loading is investigated. The analytical elastic static buckling load of the column using the Euler equation⁸⁾ is 14.9kips(66.38kN). The constant value of load, $P=15$ kips(66.72kN), is applied. The lateral deflection at the mid height of the column versus time curve (histogram) is plotted in Fig. 3.

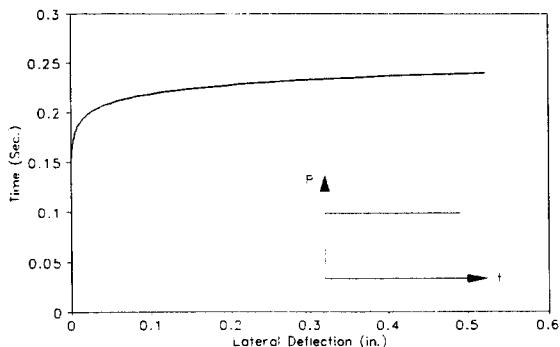


Fig. 3 Lateral displacement versus time curve for Euler column under static loading

The figure shows that the lateral deflection of column increases dramatically after 0.2sec. This behavior is assumed to indicate buckling of the column. However, the load value which causes buckling of the column cannot be determined using the histogram.

To approximate the static buckling load of the column, the load is applied using the prescribed loading rate. The column is loaded by using a linear load-time function, at which an arbitrarily determined loading rate is 6.67×10^4 lb/sec(296.68kN/sec). For an infinitesimal scale of the deflection, the load-deflection curve of the column is plotted in Fig. 4. It can be seen that prior to the load reaches the static

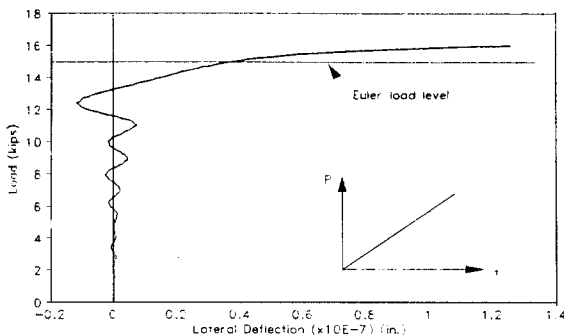


Fig. 4 Load-deflection curve for a perfect column under pseudo-static loading

buckling load level, the lateral deflection of the column oscillates. The amplitude of lateral oscillation is less than 2.0×10^{-8} inch. The previous research has indicated that a perfect column is known to develop lateral oscillation if its stable equilibrium is disturbed.⁹⁾ Once the load reaches its critical value, the amplitude of vibration begins to grow without limit. The load level $P=16$ kips can be considered as the ultimate loading capacity of the column.

4.2 Free Vibration of Euler Column

For a very short duration of impact load, free vibration of a column caused by an impact load is studied to determine the natural frequency of Euler column. The ramp shaped impact load, which is shown in Fig. 6(a), having a very short duration of 1.0×10^{-3} sec is applied laterally at the mid height of the column and removed shortly. The maximum magnitudes of load, 0.05 kips (222.4 N) and 0.1 kips (444.8 N) at half the load are considered. Upon removal of the impact load, the response is due to free vibration. The natural frequency of this column, $\omega_n = 356.48$ rad/sec, is obtained using the stiffness matrix method with the consistent mass matrix.

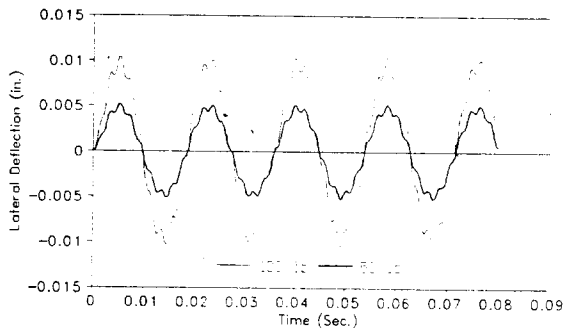


Fig. 5 Free vibration response of a column under impact loading

In Fig. 5, the lateral deflection at the mid height of the column is plotted against time. It can be seen that the frequencies of column responses are almost identical with the natural frequency of the column, regardless of the magnitudes of impact loads.

4.3 Euler Column under Impact Loading

Among the problems of the dynamic instability of structures, probably the best known problem is that under impact loading. As shown in Fig. 6, the ramp, triangular, and one half sine shaped of impulsive loadings, which have various load durations and magnitudes, are considered. In this study, the dynamic buckling response of structures subjected to impulsive loadings is investigated by considering the following loading parameters: (1) the shape; (2) magnitude; and (3) duration of impact loads.

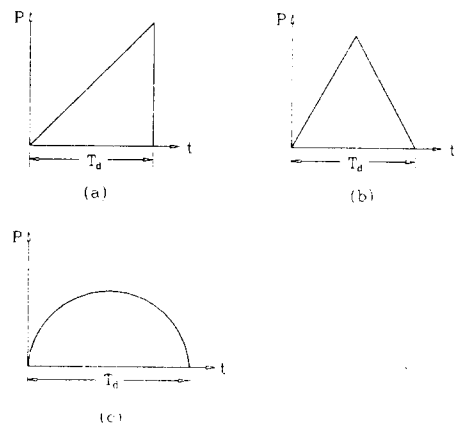


Fig. 6 Impulsive loads: (a) ramp phase; (b) triangular phase; and (c) half sine wave phase

4.3.1 Influence of load shape on column response

The sine (one half sine wave) and triangular shaped impact loads are considered. For both load shapes, the load duration is assumed to be

the same as that of the first free vibration. The first duration of free vibration, which is denoted as T_n , is 1.762×10^{-2} sec. The maximum magnitude of load 15kips(66.72kN) at half the load is assumed.

In Fig. 7, the lateral deflection at the mid height of the column is plotted against time. The figure shows that the frequencies of response due to both load shapes are almost the same. However, the maximum amplitude due to the sine shaped impact load is approximately 1.8 times larger than that of the triangular shaped load. This is because the energy produced by external load of the sine shaped load is greater than that of the triangular shaped load. On the basis of the maximum response, the sine shape is obviously severe loading case.

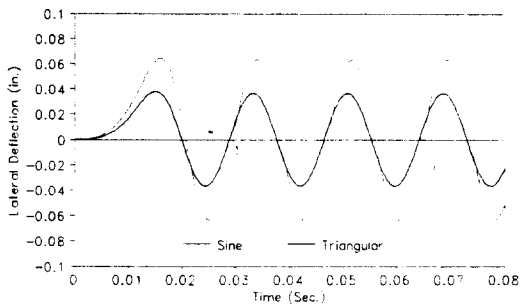


Fig. 7 Influence of load shapes on column response(constant load duration and magnitude)

4.3.2 Influence of load magnitude on column response

Since the sine shaped impact load is known as a severe loading case in the previous example, this load shape is considered. The duration of applied load, T_d , is the same as that of first free lateral vibration of the column.

In Fig. 8, for the maximum load magnitude of 5kips(22.24kN), 10 kips(44.48kN) and 15kip

s(66.72kN), the lateral deflection at the mid height of the column is plotted against time. The figure shows that the influence of the magnitudes of impact load on column response is apparent.

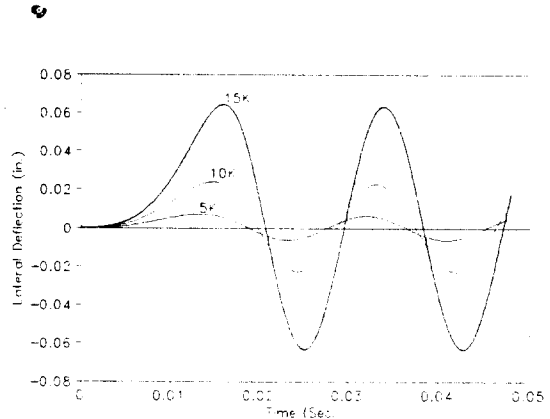


Fig. 8 Influence of load magnitudes on column response (sine shaped load and constant load duration)

As it is expected, the maximum response increases as the load magnitude increases. However, the response is not linearly proportional to the magnitude of the load. This may be due to the fact that, at a certain load magnitude, the buckling of the column influences the maximum response.

4.3.3 Influence of load duration on column response

The impact load is the sine shaped, for which the maximum magnitude of load is 15kips (66.72kN) at half the load. In the analysis, the magnitude of the load is unchanged, but load durations are changed to obtain the response curves for various load durations. Each load duration is normalized to the first period of free vibration of unloaded column, and denoted as T_d/T_n in the figure.

Fig. 9 shows the column response curves for

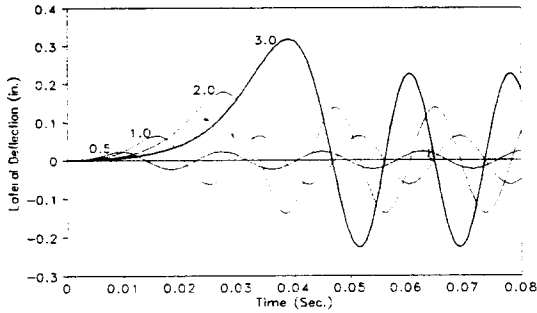


Fig. 9 Influence of load durations on column response (sine shaped load and constant load magnitude) -Deflection versus time curves for $T_d/T_n=0.5, 1.0, 2.0$ and 3.0

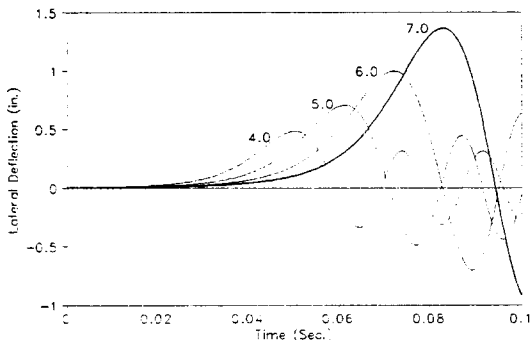


Fig. 10 Influence of load durations on column response (sine shaped load and constant load magnitude) -Deflection versus time curves for $T_d/T_n=4.0, 5.0, 6.0$ and 7.0

which $T_d/T_n=0.5, 1.0, 2.0$, and 3.0 . Fig. 10 shows the column response curves for which $T_d/T_n=4.0, 5.0, 6.0$, and 7.0 . Both figures show that the influence of load durations on column response is apparent. For relatively short load durations ($T_d/T_n < 3.0$), the dynamic effect is less than the static effect. This is because the column needs not be damaged by the impact load if the load is removed after a sufficiently short time. However, as the load duration increases, the dynamic effect is pronounced. For the impact load with $T_d/T_n=7.0$, the max-

imum response of the column is 3.5 times larger than that of static load. It is recognized that the dynamic instability is greatly influenced by the load duration. The value of $T_d/T_n=4.0$ is assumed to be the critical value of the dynamic instability for the given column.

5. CONCLUSIONS

Dynamic buckling response of columns is quite different from the corresponding static response. However, depending upon the interacting factors of dynamic analysis, dynamic effect may be less than that of the static. Based on the current findings, the relationships between the dynamic loading parameters, which influence the dynamic buckling response of columns, are summarized in the followings.

(1) The results of example problems indicate that the influence of the time variation of impulsive loading on column response is obvious. For the shapes of impulsive loading considered herein, the shape of one half sine wave load is identified as a severe loading case. In general, the maximum response due to the sine wave phase load is about two times larger than that of triangular phase of load.

(2) In addition to the time variations, the numerical results of the present study indicate that the amplitude of dynamic response of column is not proportional to the magnitude of impulsive loading. The maximum dynamic responses are abruptly increased as the load magnitudes are increased.

(3) For a short duration of impact load, the dynamic effect is less than the static effect. However, as the load duration increases, the dynamic effect becomes pronounced. For a certain case, dynamic effect on the maximum response is found to be as much as 3.5 times lar-

ger than that of static. It is therefore concluded that, where appropriate, the dynamic nature of loads must be considered in the structural problems to provide adequate safety against dynamic structural instability.

(4) Besides column examples, the dynamic buckling behavior of structural plane frames under impact loading is studied but not presented in this paper. The influence of dynamic loading parameters on frame response is similar to that of the column.

References

1. Yener, M. and Li, G. C., "Progressive Finite Element Fracture Analysis of Pullout Concrete," *J. Str. Engr., ASCE*, 117(8), 2351-2371, 1991.
2. Belytschko, T. and Hsieh, B. T., "Non-linear Transient Finite Element Analysis with Convected Coordinates," *Int. J. Num. Meth. Engr.*, 7, 255-271, 1973.
3. Bathe, K. J., *Finite Element Procedures in Engineering Analysis*, Prentice-Hall, Inc., N.J., 1982.
4. Cook, R. D., Malkus, D. S. and Plesha, M. E., *Concepts and Applications of Finite Element Analysis*, 3rd Ed., John Wiley & Sons, Inc., New York, N.Y., 1989.
5. Housner, G. W. and Tso, W. K., "Dynamic Behavior of Supercritically Loaded Struts," *J. Engr. Mech. Div., ASCE*, 88(5), 41-65, 1962.
6. Fung, Y. C., *Foundations of Solid Mechanics*, Prentice-Hall, Inc., N.J., 1965.
7. Yener, M. and Kim, H. Y., Predictive Dynamic Instability Analysis of Structural Steel Frame, *CEE Dept. Technical Report*, Utah State University, 1994.
8. Timoshenko, S. P. and Gere, J. M., *Theory of Elastic Stability*, 2nd Ed. McGraw-Hill Book Co., Inc., New York, N.Y., 1961.
9. Hoff, N. J., "Dynamic Stability of Structures," *Proc. of Int. Conf. on Dynamic Stability of Structures*, 7-41, Pergamon Press, 1967.

(접수일자 : 1996. 7. 26)